Imaging the Distribution and Secondary Structure of Immobilized Enzymes Using Infrared Microspectroscopy

ARTICLE *in* BIOMACROMOLECULES · JANUARY 2003

Impact Factor: 5.75 · DOI: 10.1021/bm025611t · Source: PubMed

4 AUTHORS, INCLUDING:

Wei Gao
Dow Chemical Company
31 PUBLICATIONS **815** CITATIONS
SEE PROFILE

Richard Gross
Polytechnic Institute of New York University
140 PUBLICATIONS **4,640** CITATIONS
SEE PROFILE

Imaging the Distribution and Secondary Structure of Immobilized Enzymes Using Infrared Microspectroscopy

Ying Mei,[†] Lisa Miller,[‡] Wei Gao,[†] and Richard A. Gross*,[†]

NSF I/UCRC for Biocatalysis and Bioprocessing of Macromolecules, Polytechnic University, Six MetroTech Center, Brooklyn, New York 11201, and National Synchrotron Light Source, Brookhaven National Laboratory, Upton, New York 11973

Received July 8, 2002; Revised Manuscript Received September 18, 2002

Synchrotron infrared microspectroscopy (SIRMS) was used for the first time to image the distribution and secondary structure of an enzyme (lipase B from *Candida antarctica*, CALB) immobilized within a macroporous polymer matrix (poly(methyl methacrylate)) at 10 μm resolution. The beads of this catalyst (Novozyme435) were cut into thin sections (12 μm). SIRMS imaging of these thin sections revealed that the enzyme is localized in an external shell of the bead with a thickness of 80−100 μm. Also, the enzyme was unevenly distributed throughout this shell. Furthermore, by SIRMS-generated spectra, it was found that CALB secondary structure was not altered by immobilization. Unlike CALB, polystyrene molecules of similar molecular weight diffuse easily throughout Novozyme435 beads. Scanning electron micrograph (SEM) images of the Novozyme435 beads showed that the average pore size is 10 times larger than CALB or polystyrene molecules, implying that there is no physical barrier to enzyme or substrate diffusion throughout the bead. Thus, the difference between polystyrene and enzyme diffusivity suggests that protein−matrix and protein−protein interactions govern the distribution of the enzyme within the macroporous resin.

Introduction

Enzymes catalyze a plethora of reactions with high specificity, speed, and yield. However, to be useful as industrial biocatalysts, improvements in enzyme stability, activity, and recovery are necessary. Traditionally, these obstacles have been addressed by the immobilization of enzymes on polymer or ceramic matrixes. A critical parameter in the performance of an immobilized enzyme is the spatial distribution of the enzyme and substrate within a macroporous resin.[1,2] The enzyme distribution has been obtained experimentally by coupling microscopic techniques with staining,[3,4] radioactive labeling,[5,6] or fluorescence labeling.[7−9] The nonuniformity of protein-labeling methods is a potential source of error in these studies. Fluorescence labeling alters the enzyme structure, which can change protein adsorption and other physicochemical properties. Staining and fluorescence labeling can cause irreversible changes to enzyme activity. In addition, a quantitative determination of protein distribution is often complicated because of the need to correlate these experiments by mathematical simulations.[7−9] In this paper, we report a novel method that allows quantitative determination of an immobilized protein's spatial distribution throughout the internal structure of a polymer bead without the need for protein modification or staining. Because this method is based on infrared spectroscopy, information on the bound protein's secondary structure was also determined.

Novozyme435 is a commercially available heterogeneous biocatalyst that consists of lipase B from *Candida antarctica* (CALB) immobilized within a macroporous resin of poly(methyl methacrylate) (Lewatit VP OC 1600). Furthermore, Novozyme435 is well recognized for its extraordinary ability to provide very high regioselectivity during the esterifications of sugars,[10] nucleosides,[11] and steroids.[12] Moreover, Novozyme435 is highly enantioselective for the resolution of secondary alcohols via hydrolysis[13] or esterification [14] in organic solvents.[15] For example, Novozyme435 has been used to prepare pure [*S*]-(+)-2-arylpropionic acids that have anti-inflammatory effects.[16] Also, Novozyme435 is effective for the build-up of polymer chains from various lactones and activated diacid/diol substrates.[17]

Infrared spectroscopy is a widely used technique for identifying the chemical makeup of materials. Depending on the type(s) of chemical bonds present in a material, infrared light is absorbed at different frequencies, yielding a unique infrared spectrum. When coupled to special microscope optics, infrared spectroscopy can be performed on very small samples in a spatially resolved fashion. Recently, the spatial resolution of infrared microspectroscopy (IRMS) has been dramatically improved by taking advantage of the high brightness of a synchrotron infrared source.[18] Thus, sample areas that are too small to be analyzed with a conventional thermal (globar) source can now be examined in detail. This improvement has proven especially valuable for applications to biological systems.[19] In this study, we took advantage of the high resolution of a synchrotron IR source to study CALB immobilized within a macroporous Lewatit VP OC 1600 resin at a spatial resolution of 10 μm. Using IR spectral signatures unique to CALB, we imaged the distribution and secondary structure of the enzyme. In

[†] Polytechnic University.
[‡] Brookhaven National Laboratory.

10.1021/bm025611t CCC: $25.00
Published on Web 10/31/2002

addition, because the IR absorbance spectrum of a model substrate (polystyrene) differs from that of CALB and the polymer bead, we simultaneously imaged and compared the diffusion of this substrate throughout the polymer matrix.

Experimental Protocol

Materials. Novozyme435 beads were a gift from Novozymes (Denmark). Lewatit VP OC 1600 resin is a product from Bayer and was a gift from Novozymes (Denmark). CALB protein solution (SP 525) was a gift from Novozymes. It was lyophilized, and then for the IR spectrum of free CALB, 2 mg of lyophilized protein was dissolved in 5 μL of water. The solution was deposited on a diamond disk (2 mm diameter $\times$ 1 mm thick) and dried as a protein film. Paraffin wax (Tissue-Tek) was obtained from Electron Microscopy Sciences. Monodisperse polystyrene standards were purchased from Aldrich Chemical Co. To study the distribution of polystyrene within Novozyme435, the Novozyme435 beads (10 mg) were incubated at 70 °C for 2 h in 0.2 mL of toluene-d_8 with 50% w/v of polystyrene.

Sample Embedding. To probe the penetration depth of CALB into the polymer bead, Novozyme435 beads were embedded in paraffin wax and the blocks were sectioned at a thickness of 12 μm using a stainless steel blade on a cryomicrotome (IEC) at room temperature. Sections were mounted on BaF_2 disks (13 mm diameter $\times$ 1 mm thick; Spectral Systems) and placed in a standard FTIR slide mount (Thermo Spectra Tech) for data collection.

Infrared Microspectroscopy. IR microspectra were recorded using a Continuμm infrared microscope equipped with a motorized $x-y$ stage and an MCT-A* detector (Thermo Nicolet). The IR microscope was coupled to a Magna 860 FTIR spectrometer and synchrotron light was used from Beamline U10B at the National Synchrotron Light Source, Brookhaven National Laboratory. A digital camera was mounted to the microscope to enable optical imaging and recording of the areas investigated. Spectra were collected in the transmission mode from 4000 to 750 cm^{-1} with 128 scans per point and 4 cm^{-1} resolution. The redundant aperture was set to 10 $\times$ 10 μm^2, and sequential spectra were collected in 10 μm steps.

Data Analysis. All spectra were collected and analyzed using Atlμs software (Thermo Nicolet). To correct for variations in synchrotron beam current, a linear baseline correction was performed on each spectrum. The enzyme distribution was calculated by plotting the peak height of the amide I band (1640 cm^{-1}), which is proportional to the enzyme concentration. Although absolute protein concentrations were not determined here, it should be noted that IR spectroscopy is a quantitative technique, so given the sample thickness, the absolute protein concentration can be determined using Beer's Law.[20] Enzyme structure was determined by curve fitting (Grams32, Galactic Industries) of the amide I band into its respective secondary structure components. The center position for each amide I subpeak was determined on the basis of previous assignments[20,21] and confirmed by using second-derivative peak analysis. All peaks were fitted by a Gaussian function with the center position limited to

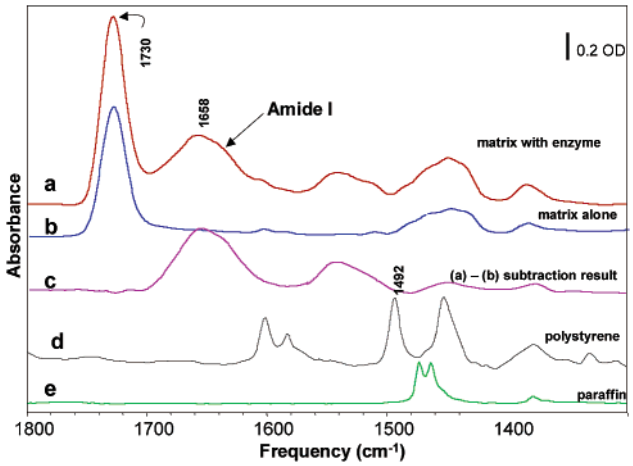

Figure 1. FTIR spectra of the Novozyme435 polymer bead (a) with enzyme and (b) without enzyme, (c) the subtraction result of a $-$ b, (d) the infrared spectrum of polystyrene, and (e) the infrared spectrum of paraffin.

$\pm$2 cm^{-1} from the initial position and the width limited to 25 cm^{-1} to avoid alternative convergent solutions. The polystyrene substrate distribution was determined by plotting the peak height at 1492 cm^{-1}. Three-column ascii data (x, y, intensity) were imported into Microcal Origin for plotting.

Scanning Electron Micrographs (SEM). Samples were applied to carbon-coated specimen stubs and coated with 10 nm Au/Pd in an argon field (BalTec MED020, Fohrenweg, Liechtenstein). Images were obtained by field-emission scanning electron microscopy (AMRAY 1910, KLA-Tencor, Beford, MA) at an accelerating potential of 5 kV and working distance of 15 mm. Digitized images were brought into Adobe Photoshop 6.0 for assembly.

Results and Discussion

IR microspectroscopy has several advantages over other techniques for analyzing immobilized enzyme distributions. First, unlike staining, fluorescence, or radiolabeling, the technique does not require the addition of a tagging agent. Second, IR microspectroscopy is quantitative, so protein concentrations can be determined if the thickness of the sample is known. Third, IR microspectroscopy not only provides enzyme distribution and concentration information but also can give information on the secondary structure of the immobilized enzyme.

To use IR microspectroscopy to probe enzyme distribution and secondary structure, the spectra of the enzyme, matrix, and other substances to be studied must each have unique features. Figure 1 illustrates the FTIR microspectra of (a) the matrix after CALB immobilization, (b) the Lewatit matrix, (c) the subtraction result of a $-$ b, (d) polystyrene, and (e) the paraffin embedding compound. The IR spectrum of CALB is dominated by the amide I and amide II bands, centered at 1660 and 1545 cm^{-1}, respectively. The amide I band is due to the stretching vibrations of the C═O bonds in the backbone of the protein; thus, the frequency of this peak is sensitive to protein secondary structure.[20,21] The amide II band arises from a combination of C$-$N stretching

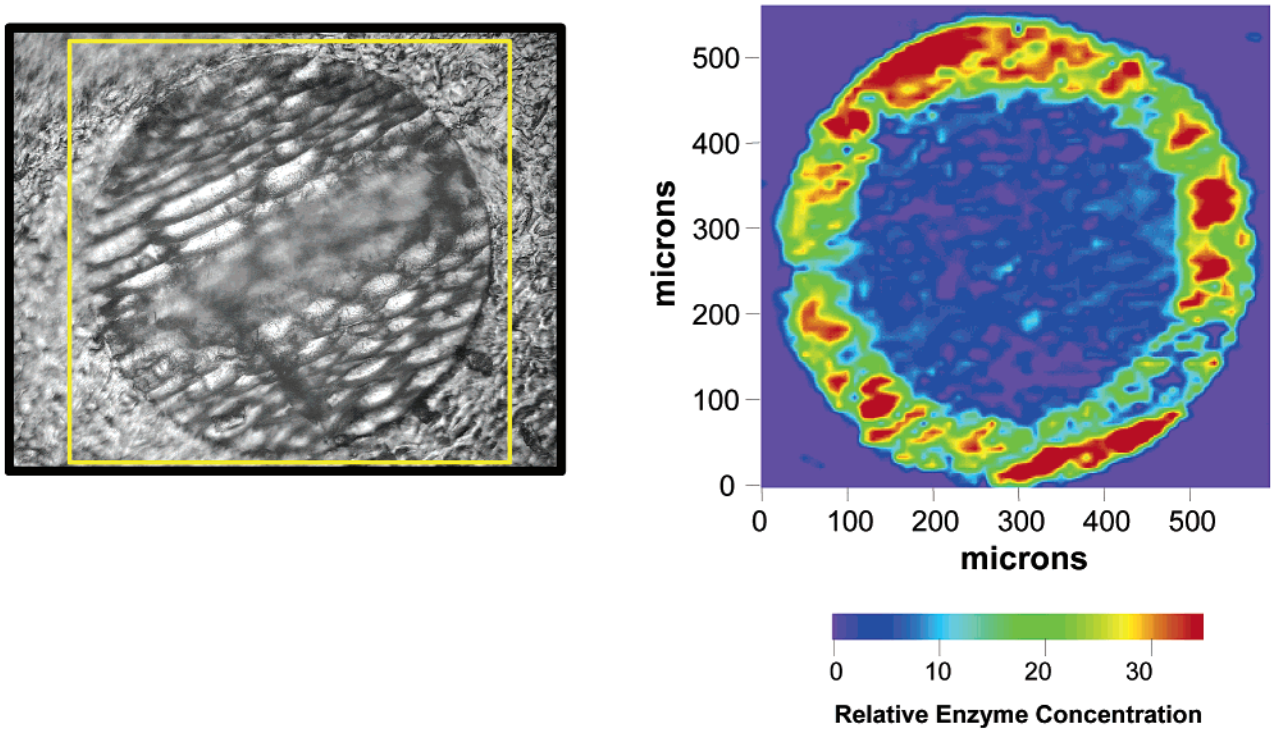

Figure 2. Visible light image (left) of the Novozyme435 bead embedded in paraffin and cross-sectioned at a 12-μm thickness. The yellow box indicates the area imaged by the IR microscope. The right panel shows the enzyme distribution throughout the center section of the Novozyme435 bead.

and N−H bending vibrations of the protein backbone.[20,21] For the bead matrix, the C═O bonds of the poly(methyl methacrylate) absorb between 1700 and 1770 cm^{-1}, which is different than the absorbance features of the enzyme. For polystyrene, an aromatic C−C stretching mode from 1449 to 1494 cm^{-1} distinguishes it from enzyme and matrix. It is also important to note that the absorbance spectrum of the paraffin embedding compound (Figure 1e) does not interfere with the spectrum of the enzyme.

On the basis of the differences between CALB and the bead matrix spectrum, the distribution of protein in the thin sections was determined. IR microspectra were collected in an automated fashion by stepping the sample in a grid-like pattern in 10 μm increments through the IR beam (10 × 10 μm^2 in size) and acquiring a spectrum at each "pixel" location. From these maps, the height of the amide I band was calculated at each pixel location to generate a contour plot of the enzyme distribution (Figure 2). This IR image shows that the protein is localized in an external shell of the bead with a thickness of 80−100 μm. Furthermore, the nonuniform image density demonstrates that the distribution of CALB is nonuniform throughout this shell.

Earlier studies suggested that restricted diffusion might greatly influence the enzyme immobilization process, especially when the characteristic size of the enzyme is similar to the pore size of the support.[22] Because the diameter of a single enzyme molecule is <10 nm,[23] scanning electron micrograph (SEM) images of similar beads were taken to assess the actual pore size of the beads. Figure 3 showed that the average pore size in Novozyme435 beads is about 100 nm, more than 10 times larger than the size of the CALB molecule. Thus, it is unlikely that a simple physical barrier prevents the diffusion of the enzyme into the core of the bead. Interestingly, Bosley and co-workers found that, for unrestricted access of the protein into the matrix, the pores must have a diameter that is approximately 4 to 5 times that of the enzyme.[24] Alternatively, we suggest that the strong affinity of CALB for the matrix and the low affinity or even repulsion between immobilized CALB molecules at the resin surface and soluble CALB limits the extent that soluble CALB reaches and adsorbs to the internal portions of the bead. In this case, longer CALB incubation times or higher concentrations of soluble CALB or both will be necessary during the immobilization process to increase the depth of penetration of CALB within the bead and, therefore, the size of the outer-shell region that contains CALB. In fact, in studies underway in our laboratory to regulate the thickness of the protein outer shell, we found that, by increasing the time for diffusion and concentration of CALB, we obtained Lewatit VP OC 1600 beads containing protein distributed throughout (unpublished results).

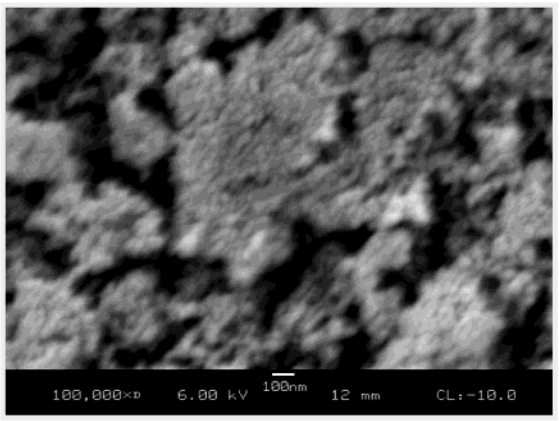

Figure 3. SEM image of the center section of Novozyme435 beads.

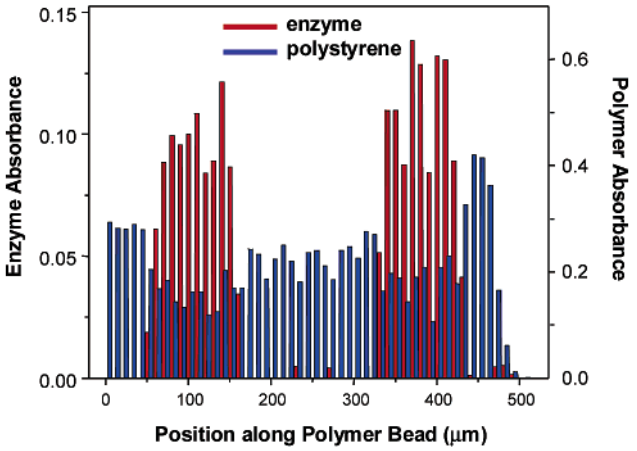

Figure 4. The distribution of enzyme and polystyrene (M_w = 46 kD, M_w/M_n = 1.05) in a Novozyme435 bead obtained by collecting an infrared line map through a Novozyme bead cross section. The bead diameter was ~400 μm. The enzyme penetrated ~100 μm into the bead, whereas polystyrene diffused throughout the entire bead.

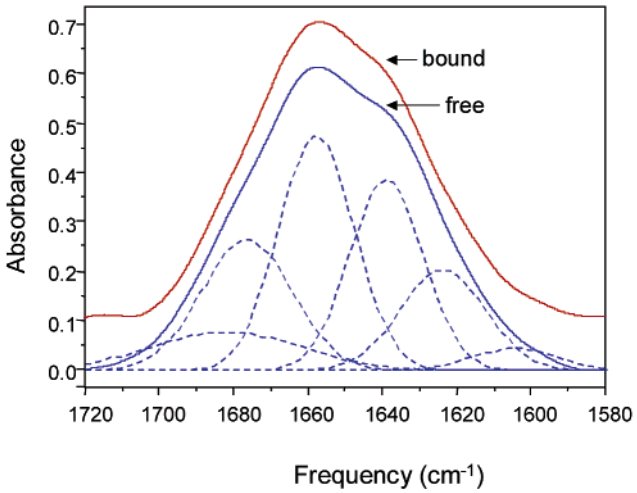

Figure 5. Curve-fit result of the amide I band of the unbound lipase B from *Candida antartica* indicating the secondary structure of the protein. The structure does not change when CALB is physically adsorbed to the polymer bead.

A complete and uniform distribution of the immobilized enzyme throughout the bead is only beneficial if catalysis can occur throughout the bead volume. To test whether the enzyme "shell" inhibits diffusion of substrate into the matrix, a concentrated solution of a model substrate (polystyrene, M_w = 46 kD, M_w/M_n = 1.05) was incubated with Novozyme435 beads in toluene-d_8 for 120 min. The molecular weight of the polystyrene (46 kD) was chosen to be slightly larger than that of CALB (33 kD). Toluene is a good solvent for polystyrene and, therefore, was selected to avoid preferential adsorption or even precipitation of polystyrene at the protein/matrix region of the beads. IR imaging shows that polystyrene is distributed uniformly throughout the beads (Figure 4). Similar results were observed for polystyrene of smaller (2, 5 and 10 K) molecular weights. Thus, there does not appear to be a physical or chemical barrier preventing the diffusion of the substrate throughout the polymer bead, suggesting that catalysis is possible throughout the bead volume.

In addition to protein distribution, the structure of the immobilized enzyme is critical to the catalytic process. Immobilization of enzymes at solid surfaces can cause a change in the enzyme conformation.[25] It is known that the amide I band of proteins (1600−1700 cm^{-1}) is sensitive to secondary structure, where α-helices, β-sheets, β-turns, and extended coil structures absorb at different frequencies.[20,21] Thus, by curve-fitting the amide I band of the CALB enzyme throughout the IR image, we can determine the secondary structure distribution. Figure 5 illustrates the curve-fitting result of soluble (nonimmobilized) CALB. On the basis of the peak frequencies and intensities of the bands, the results show that free CALB contains ~31% α-helix and ~19% β-sheet, which agrees with the published X-ray crystallographic data.[26] The IR spectra of immobilized and free CALB were indistinguishable. Moreover, the spectrum does not change as a function of the penetration depth in the bead (data not shown). Thus, immobilization of CALB within the bead did not cause a change in its conformation to an extent that can be detected by IR analysis.

In summary, IR microspectroscopy is a powerful and noninvasive method for determining the distribution and structure of immobilized enzymes. In this work, IR imaging shows that CALB is localized in an external shell of the Lewatit bead with a thickness of 80−100 μm. SEM showed that the average pore size in Novozyme435 beads is about 100 nm, more than 10 times larger than the size of the CALB molecule, indicating that it is unlikely that a simple physical barrier prevents the diffusion of the enzyme into the core of the bead. Conversely, polystyrene molecules of a similar molecular weight to CALB diffuse easily throughout the Novozyme435 beads. These results suggest that immobilization of the CALB on the Lewatit polymer matrix involves a strong affinity of the enzyme for the matrix or protein−protein interactions with other CALB molecules or both. The extent that this matrix−enzyme architecture influences the observed kinetics of CALB-catalyzed transformations is a subject for further study. Moreover, the ability of IR microspectroscopy to determine the structure of an enzyme in the immobilized state will be of value to better understand how different solid supports, solvents, and reaction conditions influence enzyme conformation−activity relationships.

Acknowledgment. We are grateful to the members of the NSF I/UCRC for Biocatalysis and Bioprocessing of Macromolecules at the Polytechnic University for their financial support of this research. The National Synchrotron Light Source (NSLS) is supported by the U.S. Department of Energy under contract No. DE-AC02-76CH00016. We thank Dr. William J. L'Amoreaux for assistance with scanning electron microscopy.

References and Notes

(1) Wang, J.; Varna, A. *Chem. Eng. Sci.* **1980**, *35*, 613−617.
(2) Aires, R. *The mathematical theory of diffusion and reaction in permeable catalysts*; Clarendon Press: Oxford, U.K., 1975.
(3) Carleysmith, S. W.; Eames, M. B. L.; Lilly, M. D. *Biotechnol. Bioeng.* **1980**, *22*, 957−967.
(4) Mosbach, K. *Sci. Am.* **1986**, *224*, 26−31.
(5) David, G. S.; Chino, T. H.; Reisfeld, R. A. *FEBS Lett.* **1974**, *43*, 264−266.
(6) Stage, D. E.; Mannik, M. *Biochim. Biophys. Acta* **1974**, *343*, 382−389.

(7) Lasch, J.; Kuhnau, R. *Enzyme Microb. Technol.* **1986**, *8*, 115−119.
(8) Mullon, C. J. P.; Saltzman, W. M.; Langer, R. *Biotechnology* **1988**, *6*, 927−929.
(9) Ladero, M.; Santos, A.; Garcia-Ochoa, F. *Biotechnol. Bioeng.* **2001**, *72*, 458−467.
(10) Kirk, O.; Bjorkling. F.; Godtredsen, S. E.; Larsen, T. O. *Biocatalysis* **1992**, *6*, 127−134.
(11) Moris, F.; Gotor, V. *J. Org. Chem.* **1993**, *58*, 653−660.
(12) Bertonotti, A.; Carra, G.; Ottolina, G.; Riva, S. *Tetrahedron* **1994**, *50*, 13165−13172.
(13) Hansen, T. V.; Waagen, V.; Partli, V.; Anthosen, H. W.; Anthosen, T. *Tetrahedron: Asymmetry* **1995**, *6*, 499−504.
(14) Frykman, H.; Ohmer, N.; Norin, T.; Hult, K. *Tetrahedron Lett.* **1993**, *34*, 1367−1370.
(15) Arroyo, M.; Sanchez-Montero, J. M.; Sinisterra, J. V. *Enzyme Microb. Technol.* **1999**, *24*, 3−12.
(16) Arroyo, M.; Sinisterra, J. *J. Org. Chem.* **1994**, *59*, 4410−4417.
(17) Gross, R. A.; Kumar, A.; Kalra, B. *Chem. Rev.* **2001**, *101*, 2097−2124.
(18) Reffner, J. A.; Martoglio, P. A.; Williams, G. P. *Rev. Sci. Instrum.* **1995**, *66*, 1298−1302.
(19) Miller, L. M.; Carr, G. L.; Jackson, M.; Williams, G. P.; Dumas, P. *Synchrotron Radiat. News* **2000**, *13*, 31−37.
(20) Susi, H.; Byler, D. M. *Biochem. Biophys. Res. Commun.* **1983**, *115*, 391−397.
(21) Byler, D. M.; Susi, H. *Biopolymers* **1986**, *25*, 469−487.
(22) Dennis, K. E.; Clark, D. S.; Bailey, J. E.; Cho, Y. K.; Park, Y. H. *Biotechnol. Bioeng.* **1984**, *26*, 892−900.
(23) Wannerberger, K.; Arnebrant, T. *Langmuir* **1997**, *13*, 3488−3493.
(24) Bosley, J. A.; Clayton, J. C. *Biotechnol. Bioeng*. **1994**, *43*, 934−938.
(25) Torii, H.; Tasumi, M. In *Infrared Spectroscopy of Biomolecules*; Mantsch, H. H., Chapman, D., Eds.; John Wiley & Sons: New York, 1996; pp 1−18. Krimm, S.; Bandekar, J. *Adv. Protein Chem*. **1986**, *38*, 181. Susi, H.; Byler, D. M. *Methods Enzymol*. **1986**, *130*, 290. Pancoska, P.; Wang, L.; Keiderling, T. A. *Protein Sci*. **1993**, *2*, 411.
(26) Uppenberg, J.; Hansen, M. T.; Patkar, S.; Jones, T. A. S*tructure* **1994**, *2*, 293−308.

BM025611T